Science
AAAS

Coupling Mechanics to Charge Transport in Carbon Nanotube Mechanical Resonators

Benjamin Lassagne, *et al.*

Science **325**, 1107 (2009);
DOI: 10.1126/science.1174290

small V_{sd}. In Fig. 4, we consider small or absent RF driving force and now apply a large V_{sd} across the quantum dot. Figure 4A shows a standard Coulomb blockade measurement of the quantum dot. Mechanical effects in Coulomb diamonds have been studied before in the form of phonon sidebands of electronic transitions (*25*–*28*). Shown in the data of Fig. 4 are reproducible ridges of positive and negative spikes in the differential conductance as indicated by arrows. This instability has been seen in all 12 measured devices with clean suspended nanotubes and never in nonsuspended devices. Figure 4, B and C, shows such ridges in a second device, visible as both spikes in the differential conductance (Fig. 4B) and discrete jumps in the current (Fig. 4C). The barriers in device two were highly tunable: We found that the switch-ridge could be suppressed by reducing the tunnel coupling to the source-drain leads, thereby decreasing the current. The instability disappears roughly when the tunnel rate is decreased below the mechanical resonance frequency (see SOM) (*20*).

In a model predicting such instabilities (*29*), positive feedback from single-electron tunneling excites the mechanical resonator into a large-amplitude oscillation. The theory predicts a characteristic shape of the switch-ridges and the suppression of the ridges for $\Gamma \sim f_0$, in marked agreement with our observations. Such feedback also requires a very high Q, which may explain why it has not been observed in previous suspended quantum-dot devices (*26*, *28*). If the required positive feedback is present, however, it should also have a mechanical signature; such a signature is demonstrated in Fig. 4E. The RF-driven mechanical resonance experiences a dramatic perturbation triggered by the switch-ridge discontinuities in the Coulomb peak current shown in Fig. 4D. At the position of the switch, the resonance peak shows a sudden departure from the expected frequency dip (dashed line) and becomes strongly asymmetric and broad, as if driven by a much higher RF power. This is indeed the case, but the driving power is now provided by an internal source: Because of the strong feedback, the random fluctuating force from single-electron tunneling becomes a driving force coherent with the mechanical oscillation. Remarkably, the dc current through the quantum dot can be used both to detect the high-frequency resonance and, in the case of strong feedback, directly excite resonant mechanical motion.

References and Notes

1. H. G. Craighead, *Science* **290**, 1532 (2000).
2. K. L. Ekinci, M. L. Roukes, *Rev. Sci. Instrum.* **76**, 061101 (2005).
3. K. L. Ekinci, X. M. H. Huang, M. L. Roukes, *Appl. Phys. Lett.* **84**, 4469 (2004).
4. B. Lassagne, D. Garcia-Sanchez, A. Aguasca, A. Bachtold, *Nano Lett.* **8**, 3735 (2008).
5. H.-Y. Chiu, P. Hung, H. W. Postma, M. Bockrath, *Nano Lett.* **8**, 4342 (2008).
6. R. G. Knobel, A. N. Cleland, *Nature* **424**, 291 (2003).
7. M. D. LaHaye, O. Buu, B. Camarota, K. C. Schwab, *Science* **304**, 74 (2004).
8. A. Naik *et al.*, *Nature* **443**, 193 (2006).
9. K. C. Schwab, M. L. Roukes, *Phys. Today* **58**, 36 (2005).
10. C. M. Caves, K. S. Thorne, R. W. Drever, V. D. Sandberg, M. Zimmermann, *Rev. Mod. Phys.* **52**, 341 (1980).
11. C. A. Regal, J. D. Teufel, K. W. Lehnert, *Nat. Phys.* **4**, 555 (2008).
12. A. K. Hüttel *et al.*, *Nano Lett.* **9**, 2547 (2009).
13. M. T. Woodside, P. L. McEuen, *Science* **296**, 1098 (2002).
14. J. Zhu, M. Brink, P. L. McEuen, *Appl. Phys. Lett.* **87**, 242102 (2005).
15. R. Stomp *et al.*, *Phys. Rev. Lett.* **94**, 056802 (2005).
16. G. A. Steele, G. Gotz, L. P. Kouwenhoven, *Nat. Nano.* **4**, 363 (2009).
17. V. Sazonova *et al.*, *Nature* **431**, 284 (2004).
18. B. Witkamp, M. Poot, H. S. J. van der Zant, *Nano Lett.* **6**, 2904 (2006).
19. S. Sapmaz, Y. Blanter, L. Gurevich, H. S. J. van der Zant, *Phys. Rev. B* **67**, 235414 (2003).
20. Supporting online material is available on *Science* Online.
21. C. W. J. Beenakker, *Phys. Rev. B* **44**, 1646 (1991).
22. M. Brink, thesis, Cornell Univerity (2007).
23. A. Cleland, *Foundations of Nanomechanics* (Springer, Berlin, 2002).
24. A. H. Nayfeh, D. T. Mook, *Nonlinear Oscillations* (Wiley, New York, 1979).
25. H. Park *et al.*, *Nature* **407**, 57 (2000).
26. S. Sapmaz, J. P. Herrero, Ya. M. Blanter, C. Dekker, H. S. J. van der Zant, *Phys. Rev. Lett.* **96**, 026801 (2006).
27. F. A. Zwanenburg, C. E. van Rijmenam, Y. Fang, C. M. Lieber, L. P. Kouwenhoven, *Nano Lett.* **9**, 1071 (2009).
28. R. Leturcq *et al.*, *Nat. Phys.* **5**, 327 (2009).
29. O. Usmani, Y. M. Blanter, Y. V. Nazarov, *Phys. Rev. B* **75**, 195312 (2007).

30. We thank Y. M. Blanter and Y. V. Nazarov for helpful discussions. This work was supported by the Dutch Organization for Fundamental Research on Matter, the Netherlands Organization for Scientific Research, the Nanotechnology Network Netherlands, and the Japan Science and Technology Agency International Cooperative Research Project.

Supporting Online Material

www.sciencemag.org/cgi/content/full/1176076/DC1
Materials and Methods
SOM Text
Figs. S1 to S6
References

11 May 2009; accepted 13 July 2009
Published online 23 July 2009;
10.1126/science.1176076
Include this information when citing this paper.

Coupling Mechanics to Charge Transport in Carbon Nanotube Mechanical Resonators

Benjamin Lassagne,[1]* Yury Tarakanov,[2] Jari Kinaret,[2] David Garcia-Sanchez,[1] Adrian Bachtold[1]†

Nanoelectromechanical resonators have potential applications in sensing, cooling, and mechanical signal processing. An important parameter in these systems is the strength of coupling the resonator motion to charge transport through the device. We investigated the mechanical oscillations of a suspended single-walled carbon nanotube that also acts as a single-electron transistor. The coupling of the mechanical and the charge degrees of freedom is strikingly strong as well as widely tunable (the associated damping rate is ~3 × 10^6 Hz). In particular, the coupling is strong enough to drive the oscillations in the nonlinear regime.

Carbon nanotubes have been used to fabricate mechanical resonators that can be operated at ultrahigh frequencies, have widely tunable resonance frequencies, and can be used as ultrasensitive inertial mass sensors (*1*–*10*). In addition, carbon nanotubes also have exceptional electron transport properties, including ballistic conduction over long distances or multiple Coulomb blockade–related phenomena that can be observed even up to room temperature (*11*). Coupling the mechanical motion of nanotube resonators to electron transport is thus highly appealing. In particular, we would like to use such a coupling as a way to control the mechanical motion at the nanoscale. Recently, microfabricated silicon resonators have been fabricated whose mechanical vibrations are damped by cooling from a nearby superconducting single-electron transistor (*12*). In the case of nanotube resonators, however, the extent to which it is possible to couple mechanical vibrations and charge transport is not clear.

We studied the coupling between the mechanics and the electron transport of a single-walled carbon nanotube (SWNT) resonator at cryogenic temperature in which conducting electrons enter the Coulomb-blockade regime. We show that single electrons tunneling into and out of the nanotube greatly affect the nanotube motion. The coupling can be made stronger than in nanoelectromechanical systems (NEMS) resonators studied so far, including those fabricated in silicon by using top-down approaches. Moreover,

[1]Centre d'Investigació en Nanociència i Nanotecnologia (Consejo Superior de Investigaciones Científicas–Institut Català de Nanotecnologia), campus Universitat Autònoma de Barcelona, E-08193 Barcelona, Spain. [2]Department of Applied Physics, Chalmers University of Technology, SE-41296 Göteborg, Sweden.

*Present address: Université de Toulouse, Université Paul Sabatier, Institut National des Sciences Appliquées, UMR 5215 Laboratoire de Physique et Chimie de Nano-Objets CNRS, F-31077 Toulouse, France.

†To whom correspondence should be addressed. E-mail: adrian.bachtold@cin2.es

the coupling allows us to modify the motion of the SWNT in an unprecedented manner. The resonance frequency, the quality factor, and the nonlinear dynamic can be tuned by using an external electric means (voltage applied on a gate), which is convenient for practical use.

We fabricated devices using standard nanofabrication techniques (Fig. 1A). SWNTs were grown by means of chemical-vapor deposition on a highly doped Si substrate coated with a 1-μm-thick SiO_2 layer. SWNTs were connected to two Cr/Au electrodes (5nm/100nm) by use of electron-beam lithography. We performed wet etching in buffered hydrofluoric acid so as to suspend the nanotube. An annealing treatment at 400 C during 1 hour in a flow of Ar and H_2 was carried out in order to remove impurities (polymethyl methacrylate residues and other contaminants) from the SWNTs.

The SWNT motion was driven by applying an oscillating voltage $V_g^{AC}\cos(2\pi ft)$ on the gate (Fig. 1A), which generates an electrostatic force $F_{drive} \propto V_g^{AC}\cos(2\pi ft)$ on the SWNT. The induced motion was detected via a mixing technique (*1*). For this, we applied a second voltage on the source electrode $V_{SD}^{AC}\cos[2\pi(f+\delta f)t]$. The SWNT acted as a frequency mixer, and we measured the mixing current I_{mix} at the frequency component δf from the drain electrode (Fig. 1A). The line shape of I_{mix} as a function of f (Fig. 1B) allows us to extract the resonance frequency f_0 and the quality factor Q (*13*).

Figure 2A shows the electron transport properties of the device; the SWNT differential conductance G at 4 K is plotted as a function of the constant voltage V_g^{DC} applied on the gate and the constant voltage V_{SD}^{DC} applied on the source. G oscillated with V_g^{DC} in a way that is typical of the Coulomb-blockade regime. As for the mechanical properties, Fig. 2B shows that some features of I_{mix} oscillate with V_g^{DC} with the same period as for G (such as the shape of the red lobes). The correlation between the electrical conductance and the mechanical motion becomes clearer in Fig. 3, A, C, and E, where we plot G at zero-bias, f_0, and Q as functions of V_g^{DC}. Indeed, G is the maximum, whereas f_0 and Q are low. This correlation suggests that the mechanical motion is influenced by Coulomb blockade.

Charge transport through SWNTs in the Coulomb-blockade regime is a well-studied phenomenon. When sweeping V_g^{DC}, the conductance oscillates, whereas the charge q_{dot} residing on the nanotube dot increases stepwise (Fig. 1, C and D). In our experiment, the nanotube is also behaving as a mechanical resonator (with resonance frequency f_0, effective spring constant k, and effective mass m). The capacitance C_g between the SWNT and the gate oscillates as $\delta C_g = C_g'\delta z$ (where δz is the SWNT deflection and C_g' the derivative of C_g with respect to δz). As a result, the SWNT is repeatedly charging and discharging by the amount δq_{dot}.

This charge oscillation causes damping of the mechanical motion because δq_{dot} has to flow through the tunnel resistances at the SWNT-electrode interfaces (Fig. 3B) and the energy dissipated by the current is supplied from the mechanical resonator. This dissipation is equivalent to an out-of-phase force acting on the SWNT (*13*–*15*). Consequently, the oscillating motion is delayed (by a phase $\propto 1/Q$) as compared with when no electrons are tunnelling onto the SWNT.

The oscillating charge on the SWNT also results in a shift of the resonance frequency of the resonator. The reason is that the flow of the charge modifies the electrostatic force $F_e = \frac{1}{2}C_g'(V_g^{DC} - V_{dot})^2$ between the gate and the nanotube (V_{dot} is the nanotube potential and depends on δq_{dot}). Indeed, it can be shown that F_e oscillates as a spring force (*13*). This modifies the spring constant of the SWNT resonator by δk. The resonator softens or hardens, and the resonance frequency changes by the amount $\delta f_0 = f_0/2 \cdot \delta k/k$.

This damping and the resonance frequency are expected to oscillate with V_g^{DC} because the amplitude of the δq_{dot} oscillation depends on V_g^{DC} (the amplitude is large when q_{dot} increases sharply with V_g^{DC} and low when q_{dot} increases weakly with V_g^{DC}) (Fig. 1C, green segment). Q and δf_0 can be expressed as (*13*)

$$1/Q = 2\pi f_0 \frac{C_g'^2}{k}(V_g^{DC})^2\left(\frac{2}{\Gamma C_{dot}}\right)^2 G \quad (1)$$

$$\delta f_0 = -\frac{f_0}{2}\frac{C_g'^2}{k}\frac{(V_g^{DC})^2}{C_{dot}}\left(\frac{2G}{C_{dot}\Gamma} - 1\right) \quad (2)$$

where Γ is the tunnelling rate through the nanotube-electrode interface and C_{dot} is the total dot capacitance. Equation 1 and 2 are valid for $f_0 << \Gamma$ and in the so-called quantum regime of Coulomb blockade, in which the thermal energy k_BT (where k_B is Boltzmann's constant and T is the temperature) is lower than the level spacing (the energy separation due to quantum confinement). Equations 1 and 2 show that Q and f_0 oscillate as a function of V_g^{DC} with the same period as for G, which is in agreement with the experiments. We compared the measurements to Eqs. 1 and 2 using the measured G in Fig. 3A and taking

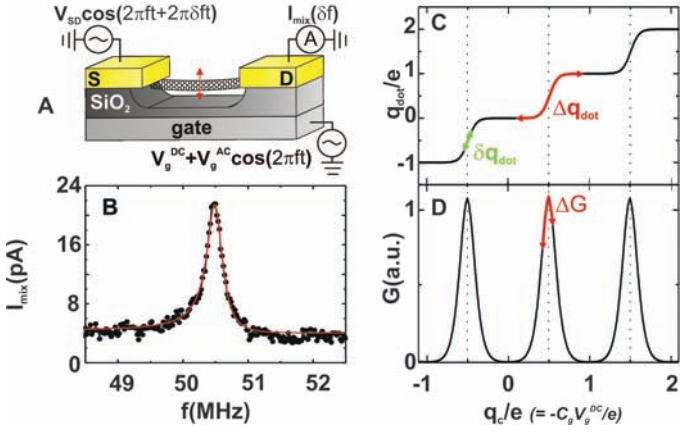

Fig. 1. (**A**) Schematic of the mechanical resonator. The moveable part is a SWNT (oscillations indicated by a red arrow). The SWNT length is 1 μm and the diameter is ~1.1 nm. The motion is capacitively driven by the application of an oscillating voltage on the gate. The nanotube position is detected by applying an oscillating voltage on the source electrode and measuring the current from the drain electrode. δf = 10 kHz. (**B**) Measured mechanical resonance (mixing current as a function of driving frequency). The red curve is a fit of the resonance. (**C** and **D**) Schematic of the charge on the SWNT and its conductance as a function of the control charge ($q_c = -C_g V_g^{DC}$) in the Coulomb-blockade regime. Vibrations cause the charge on the SWNT to oscillate (δq_{dot} and Δq_{dot}).

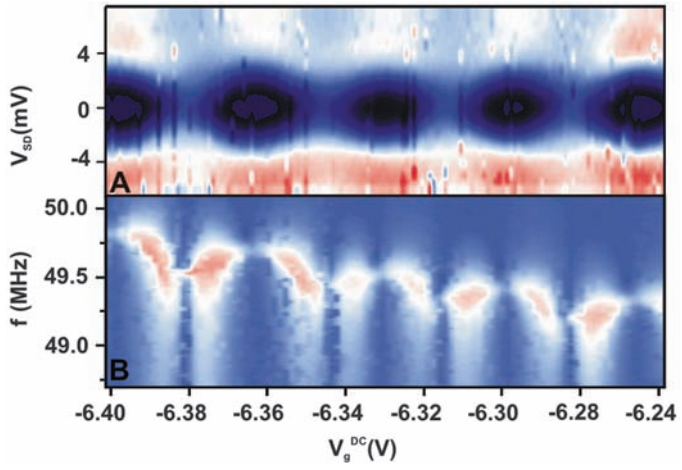

Fig. 2. Electronic and mechanical properties of the device at 4 K. (**A**) The SWNT differential conductance as a function of source-drain voltage and gate voltage. The measurements are consistent with Coulomb blockade. Blue corresponds to low conductance, and red corresponds to high conductance. (**B**) Mixing current from the drain as a function of driving frequency and gate voltage. The frequency of the red lobes (related to the mechanical resonance) goes up and down when increasing V_g^{DC} with the same period as for the SWNT conductance. This shows that the mechanics and the charge transport in the device are correlated. In addition, the frequency of the red lobes shifts continuously over the full V_g^{DC} sweep caused by mechanical tension (the static electrostatic force bends the nanotube). V_g^{AC} is 0.5 mV and V_{SD}^{AC} is 0.1 mV (f_0 and Q remain the same when decreasing V_g^{AC} to 0.15 mV at 4K). Blue corresponds to low current, and red corresponds to high current.

$C_g'^2/k$ and Γ as fitting parameters (*16*). Figure 3, D and F, shows that the agreement is rather good. The values obtained for $C_g'^2/k$ and Γ were in quite reasonable agreement with theory (*17*).

These results show that the coupling between mechanical oscillations and the charge transport is the main dissipation mechanism at low temperature in the SWNT resonator (*18*). Our work shows that an obvious fabrication strategy in the future in order to obtain higher Q at low temperature is to reduce the resistance at the SWNT-electrode interfaces ($Q \propto \Gamma$). Other dissipation mechanisms such as thermoelastic damping dominate $1/Q$ at higher temperatures. Indeed, $1/Q$ associated to the coupling between the mechanics and the electron transport is expected to be about 10^{-7} (*13*), whereas the measured $1/Q$ is 1/40.

We considered measurements in which the large driving force applied to the SWNT accesses the nonlinear dynamic of the motion. Figure 4, A and B, shows two resonance peaks at 1.5 K (mixing current as a function of driving frequency). The resonance in Fig. 4A has a surprising shape; it splits in two peaks, a broad and a narrow one. The narrow peak appears only at gate voltages near the Coulomb blockade conductance peaks (Fig. 4B, inset, and Fig. 4C). The most striking feature is that its width becomes narrower when increasing the driving force. The (effective) quality factor can increase up to about 5100 (Fig. 4E).

The coupling between the mechanics and the charge transport plays a central role in this nonlinear dynamic, as illustrated in Fig. 1C and by considering large mechanical oscillation amplitude (large oscillations of C_g). During one oscillation cycle, the charging and discharging of the dot is highly nontrivial because of the stepwise dependence of q_{dot} on V_g^{DC} (Fig. 1C, red trace Δq_{dot}). As a result, F_e depends nonlinearly on δz in contrast to the linear dependence at low oscillation amplitude. We have carried out numerical simulations to quantify this force and its effect on the motion. Specifically, the nanotube displacement and the force F_e have been calculated iteratively as a function of time in a self-consistent manner. The oscillating voltages applied on the gate and the source at frequencies f and $f + \delta f$, respectively, have been included in order to obtain the current from the drain as a function of time. A limit cycle in the simulation is obtained. Full details of our simulations are provided in (*13*). The calculations predict the appearance of an extra peak at gate voltages close to the Coulomb-blockade conductance peaks as well as a V_g^{DC} dependence of the resonance frequency that are in agreement with the experiments (Fig. 4, C and D). In addition, the simulations show that the width of the extra peak becomes narrower when increasing V_g^{AC}, but the effect is somewhat smaller than observed in the experiment (Fig. 4, E and F). Overall, it is remarkable that the calculations can capture the main experimental findings, especially when considering the simplicity of the model. The model may be improved by the incorporation of additional effects, such as mechanical-related nonlinearities that are expected to be important in SWNTs (*19*).

The double-peak structure in the simulations arises from the interplay between two nonlinear phenomena: one associated with the nonlinear dynamic of the motion (discussed above) and the other with the nonlinear detection mechanism. The latter nonlinearity becomes relevant when the amplitude of the mechanical motion is sufficient to drive G through the Coulomb blockade peak (Fig. 1D, red trace ΔG). The simulations, in that case, show that the induced current is lowered. This reduction of the current occurs only for large δz so that a resonance in position (δz as a function of f) is detected in $I_{mix}(f)$ as a double peak structure. If the shape of the resonance in δz was a Lorentzian, the two peaks in I_{mix} would have the same shape. However, the resonance in position has a sharkfin shape [Duffing-like resonance (*20*)] because of the nonlinearity of q_{dot} on δz so that one peak in I_{mix} is narrower (Fig. 4F, inset). Because the second peak

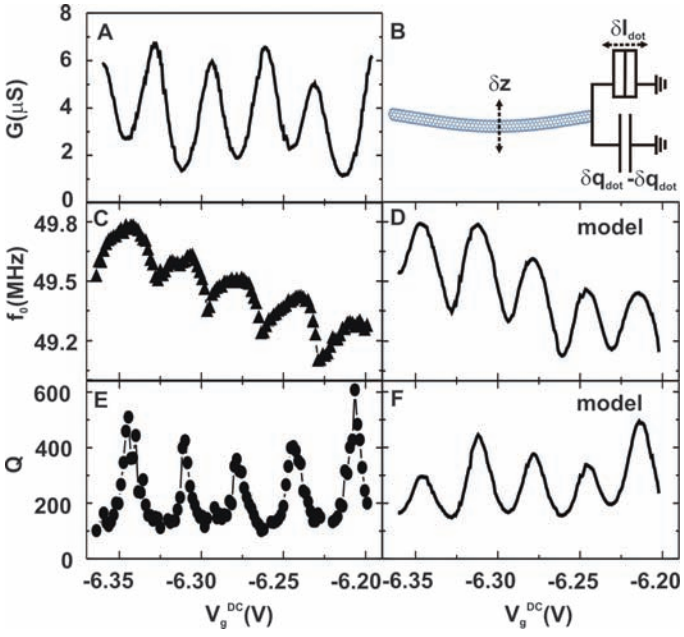

Fig. 3. Electronic and mechanical properties of the device at 4 K. (**A**) Conductance of the SWNT as a function of gate voltage. (**B**) Schematic of the dissipation process. The mechanical oscillation charges and discharges the SWNT by the amount δq_{dot}, which results in a current δI_{dot} flowing through the resistance at the nanotube-electrode interface. (**C** and **D**) Measured and calculated resonance frequency as a function of gate voltage. (**E** and **F**) Measured and calculated quality factor as a function of gate voltage.

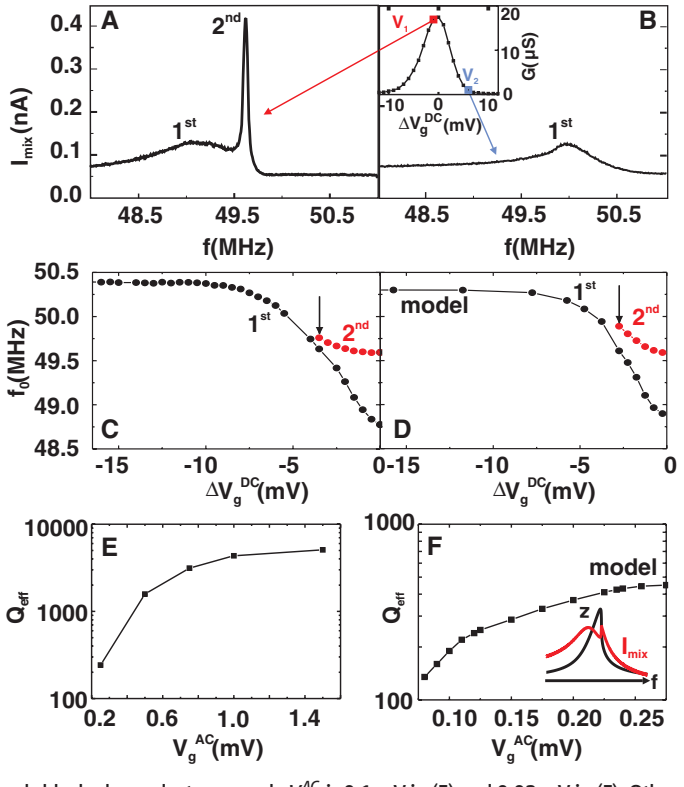

Fig. 4. Nonlinear dynamic of the SWNT motion at 1.5 K. (**A** and **B**) Mixing current as a function of driving frequency for two different gate voltages. A second peak appears in (A) that is very narrow. The inset shows the nanotube conductance as a function of gate voltage. ΔV_g^{DC} is measured from the maximum of the Coulomb-blockade peak. (**C** and **D**) Measured and calculated resonance frequency as a function of gate voltage for the two peaks. The second peak disappears at the ΔV_g^{DC} value indicated by an arrow. In (C), V_g^{AC} is 0.5 mV, and V_{SD}^{AC} is 0.1 mV. In (D), V_g^{AC} is 0.255 mV, and V_{SD}^{AC} is 0.02 mV. (**E** and **F**) Measured and calculated effective quality factor as a function of V_g^{AC} for the second peak at the Coulomb-blockade conductance peak. V_{SD}^{AC} is 0.1 mV in (E) and 0.02 mV in (F). Other parameters used in the calculations are given in (*13*). The inset shows the calculated vibration amplitude and mixing current as functions of the driving frequency.

only appears when looking at the I_{mix} signal, its high Q is only an effective quality factor, but it is useful for applications that, for instance, rely on precise measurements of the resonance frequency (*21*).

These results show that the coupling between the mechanics and the electron transport can be very strong in SWNTs. In comparison, experiments on microfabricated semiconductor resonators, which are coupled to metal single-electron transistors, have not shown any oscillations of f_0 and Q (*22*). This difference probably arises from the much greater mass of these resonators as compared with those of SWNTs, so that they are much less sensitive to the motion of individual tunneling electrons. A way to quantify the coupling is by looking at the damping rate caused by the interaction between the mechanics and the electron transport, $\gamma_{e-ph} = 2\pi f_0/Q$. Damping rate can be useful for the evaluation of quantum electromechanics phenomena in analogy to laser cooling of, for example, trapped ions (*23*). We have γ_{e-ph} as high as 3×10^6 Hz for nanotubes, which compares with $\gamma_{e-ph} \sim 0.7$ Hz for macroscopic atomic force microscopy cantilevers (*24*). As for single-electron transistors that are superconducting, γ_{e-ph} is expected to be enhanced (*15*). In this case, however, γ_{e-ph} measured on microfabricated resonators is below 5×10^4 Hz (*12*).

The strong coupling in nanotubes holds promise for various applications. We have shown that it allows for a widely tunable nonlinearity of the resonator dynamic. Nonlinearity of the motion is useful for sensitivity improvement of mass and force sensing (*25*), mechanical signal amplification (*26*, *27*), noise squeezing (*28*), study of quantum behaviors of macroscopic systems (*29*), mechanical microwave computing (*30*), or energy harvesting via vibration-to-electricity conversion (*31*). We emphasize that the nonlinearity in nanotubes can be tuned by an electronic means (by changing V_g^{DC}), which is convenient for practical use. In comparison, the nonlinearity in previously studied nanoresonators comes from purely mechanical effects (which can be described by the Duffing equation). There, the nonlinearity can be modified by using strain, but this is complicated to do experimentally. The strong coupling in nanotubes could also be used for cooling mechanical oscillations to the ground state (*32*), which would open the possibility to study nonclassical states at a mesoscopic scale. The ability to electrically tune the coupling (with V_g^{DC}) would then be very useful for quantum manipulation.

References and Notes

1. V. Sazonova *et al.*, *Nature* **431**, 284 (2004).
2. P. Poncharal, Z. L. Wang, D. Ugarte, W. A. Heer, *Science* **283**, 1513 (1999).
3. B. Reulet *et al.*, *Phys. Rev. Lett.* **85**, 2829 (2000).
4. S. T. Purcell, P. Vincent, C. Journet, V. T. Binh, *Phys. Rev. Lett.* **89**, 276103 (2002).
5. B. Witkamp, M. Poot, H. S. J. van der Zant, *Nano Lett.* **6**, 2904 (2006).
6. D. Garcia-Sanchez *et al.*, *Phys. Rev. Lett.* **99**, 085501 (2007).
7. B. Lassagne, D. Garcia-Sanchez, A. Aguasca, A. Bachtold, *Nano Lett.* **8**, 3735 (2008).
8. K. Jensen, K. Kim, A. Zettl, *Nat. Nanotechnol.* **3**, 533 (2008).
9. H.-Y. Chiu, P. Hung, H. W. C. Postma, M. Bockrath, *Nano Lett.* **8**, 4342 (2008).
10. A. Eriksson *et al.*, *Nano Lett.* **8**, 1224 (2008).
11. J.-C. Charlier, X. Blase, S. Roche, *Rev. Mod. Phys.* **79**, 677 (2007).
12. A. Naik *et al.*, *Nature* **443**, 193 (2006).
13. Materials and methods are available as supporting material on *Science* Online.
14. M. Brink, thesis, Cornell University (2007).
15. A. A. Clerk, S. Bennett, *N. J. Phys.* **7**, 238 (2005).
16. We took $C_{dot} = 57$ aF from Fig. 2A. Dissipation caused by He gas used to thermalize the resonator was included by calculating the total quality factor as $(\sum 1/Q_i)^{-1}$. The contribution of Q from He has been measured to be 1035 by means of pumping the gas, which left the temperature stable for a short moment.
17. We obtained $C_g'^2/k = 6 \times 10^{-22}$ F^2/Nm, which has to be compared with $C_g' \approx 10^{-13}$–10^{-12} F/m obtained by using commercial simulators and $k \approx 10^{-4}$–10^{-3} N/m from (*1*). The value of Γ is 3×10^9 s^{-1}, which is somewhat smaller than expected in the quantum regime $\Gamma = 8k_BTG_{max}/e^2 \approx 9 \times 10^{10}$ s^{-1} (where G_{max} is the maximum conductance of a Coulomb-blockade peak). In addition, the shape of the measured oscillations of f_0 and Q differs to some extent from what is predicted (Fig. 3). These differences may arise from the fact that the nanotube dot is not perfect (the Coulomb blockade peaks are not fully periodic in V_g^{DC}, and the peak heights are different). Another explanation is that the model that was used is too simple to quantitatively capture the physics (*33*, *34*).
18. The oscillation of Q as a function of V_g^{DC} has been observed in a second device. The Coulomb-blockade oscillations of G are, however, less regular than the ones presented here, and so the nanotube probably consists of a series of quantum dots (*35*).
19. W. G. Conley, A. Raman, C. M. Krousgrill, S. Mohammadi, *Nano Lett.* **8**, 1590 (2008).
20. L. D. Landau, E. M. Lifshitz, *Mechanics* (Pergamon Press, Oxford, 1960).
21. When V_g^{AC} is low, the values of f_0 and Q extracted from $I_{mix}(f)$ are the same as the ones from $\delta z(f)$.
22. R. G. Knobel, A. N. Cleland, *Nature* **424**, 291 (2003).
23. C. Raab *et al.*, *Phys. Rev. Lett.* **85**, 538 (2000).
24. M. T. Woodside, P. L. McEuen, *Science* **296**, 1098 (2002).
25. J. S. Aldridge, A. N. Cleland, *Phys. Rev. Lett.* **94**, 156403 (2005).
26. A. Erbe *et al.*, *Appl. Phys. Lett.* **77**, 3102 (2000).
27. R. L. Badzey, P. Mohanty, *Nature* **437**, 995 (2005).
28. R. Almog, S. Zaitsev, O. Shtempluck, E. Buks, *Phys. Rev. Lett.* **98**, 078103 (2007).
29. V. Peano, M. Thorwart, *Phys. Rev. B* **70**, 235401 (2004).
30. S. B. Shim, M. Imboden, P. Mohanty, *Science* **316**, 95 (2007).
31. F. Cottone, H. Vocca, L. Gammaitoni, *Phys. Rev. Lett.* **102**, 080601 (2009).
32. S. Zippilli, G. Morigi, A. Bachtold, *Phys. Rev. Lett.* **102**, 096804 (2009).
33. A. D. Armour, M. P. Blencowe, Y. Zhang, *Phys. Rev. B* **69**, 125313 (2004).
34. F. Pistolesi, S. Labarthe, *Phys. Rev. B* **76**, 165317 (2007).
35. B. Gao, D. C. Glattli, B. Placais, A. Bachtold, *Phys. Rev. B* **74**, 085410 (2006).

36. We thank G. Morigi and J. Moser for discussions. The research has been supported by the European Union–funded projects FP6-IST-021285-2 and FP6-ICT-028158, and the Swedish Foundation for Strategic Research.

Supporting Online Material

www.sciencemag.org/cgi/content/full/1174290/DC1
Materials and Methods

31 March 2009; accepted 19 June 2009
Published online 23 July 2009;
10.1126/science.1174290
Include this information when citing this paper.

The Chemical Structure of a Molecule Resolved by Atomic Force Microscopy

Leo Gross,[1]* Fabian Mohn,[1] Nikolaj Moll,[1] Peter Liljeroth,[1,2] Gerhard Meyer[1]

Resolving individual atoms has always been the ultimate goal of surface microscopy. The scanning tunneling microscope images atomic-scale features on surfaces, but resolving single atoms within an adsorbed molecule remains a great challenge because the tunneling current is primarily sensitive to the local electron density of states close to the Fermi level. We demonstrate imaging of molecules with unprecedented atomic resolution by probing the short-range chemical forces with use of noncontact atomic force microscopy. The key step is functionalizing the microscope's tip apex with suitable, atomically well-defined terminations, such as CO molecules. Our experimental findings are corroborated by ab initio density functional theory calculations. Comparison with theory shows that Pauli repulsion is the source of the atomic resolution, whereas van der Waals and electrostatic forces only add a diffuse attractive background.

Noncontact atomic force microscopy (NC-AFM), usually operated in frequency-modulation mode (*1*), has become an important tool in the characterization of nanostructures on the atomic scale. Recently, impressive progress has been made, including atomic resolution with chemical identification (*2*) and measurement of the magnetic exchange force with atomic resolution (*3*). Moreover, lateral (*4*) and vertical (*5*) manipulation of atoms and the determination of the vertical and lateral forces during such manipulations (*6*) have been demonstrated. Striking results have also been obtained in AFM investigations of single molecules. For example, atomic resolution was achieved on single-walled carbon nanotubes (SWNTs) (*7*, *8*), and the force needed to switch a molecular conformation was measured (*9*).

However, the complete chemical structure of an individual molecule has so far not been imaged with atomic resolution. The reasons that make AFM investigations on single molecules so challenging are the strong influence of the exact

[1]IBM Research, Zurich Research Laboratory, 8803 Rüschlikon, Switzerland. [2]Debye Institute for Nanomaterials Science, Utrecht University, Post Office Box 80000, 3508 TA Utrecht, Netherlands.

*To whom correspondence should be addressed. E-mail: lgr@zurich.ibm.com